Inorganic Chemistry

Electronic Supplementary Material (ESI)

Di(hydroperoxy)cycloalkane Adducts of Triarylphosphine Oxides: A Comprehensive Study Including Solid-State Structures and Association in Solution

Fabian F. Arp,[a] Nattamai Bhuvanesh,[a] Janet Blümel*,[a]

Received July 2020

[a] *Department of Chemistry, Texas A&M University, College Station, TX, 77842-3012, USA. Email: bluemel@tamu.edu*

X-Ray Crystallography

1. A solution of **1** in dry dichloromethane was concentrated by slow evaporation in a nitrogen stream under an inert atmosphere. A colorless block with very well-defined faces from a representative sample of crystals of the same habit was collected and data were obtained as outlined in Table **S1**. The X-ray radiation employed was generated from a Mo-Iμs X-ray tube (K_α = 0.71073 Å with a potential of 50 kV and a current of 1.0 mA). 45 data frames were taken at widths of 1.0°. These reflections were used to determine the unit cell. The unit cell was verified by examination of the *h k l* overlays on several frames of data. No super-cell or erroneous reflections were observed. After careful examination of the unit cell, an extended data collection procedure (4 sets) was initiated using omega and phi scans.

Integrated intensity information for each reflection was obtained by reduction of the data frames with the program *APEX3*.[S1] The integration method employed a three-dimensional profiling algorithm and all data were corrected for Lorentz and polarization factors, as well as for crystal decay effects. Finally, the data was merged and scaled to produce a suitable data set. The absorption correction program *SADABS* [S2] was employed to correct the data for absorption effects.

Systematic reflection conditions and statistical tests of the data were used to determine the space group. A solution was obtained readily using *XT/XS* in *APEX3*.[S1,S3] Hydrogen atoms were placed in idealized positions and were set riding on the respective parent atoms.[S4] All non-hydrogen atoms were refined with anisotropic thermal parameters.

Absence of additional symmetry and voids were confirmed using *PLATON (ADDSYM)*.[S5] The structure was refined (weighted least squares refinement on F^2) to convergence.[S3,S6] *Olex2* and *Mercury* were employed for the final data presentation and structure plots.[S6,S7]

3. A solution of **3** in a mixture of dichloromethane and hexanes (1:1) was concentrated by slow evaporation. A colorless block with very well-defined faces from a representative sample of crystals of the same habit was collected and data were obtained as outlined in Table S1, and the structure was solved as in **1**. 45 data frames

were taken at widths of 1.0°. These reflections were used to determine the unit cell. The unit cell was verified by examination of the *h k l* overlays on several frames of data. No super-cell or erroneous reflections were observed. After careful examination of the unit cell, an extended data collection procedure (6 sets) was initiated using omega and phi scans.

4. A solution of **4** in a mixture of dichloromethane and hexanes (1:1) was concentrated by slow evaporation. A colorless block with very well-defined faces from a representative sample of crystals of the same habit was collected and data were obtained as outlined in Table **S1**, and the structure was soved as in **1**. The X-ray radiation employed was generated from a Cu-X-ray sealed tube (K_α = 1.5418 Å with a potential of 50 kV and a current of 40.0 mA). 60 data frames were taken at widths of 1.0°. These reflections were used in the auto-indexing procedure to determine the unit cell. The unit cell was verified by examination of the *h k l* overlays on several frames of data. No super-cell or erroneous reflections were observed. After careful examination of the unit cell, an extended data collection procedure (3 sets) was initiated using omega scans.

Elongated ellipsoids on one *o*-Tol group (C15-C21) and the residual electron density near the group suggested disorder and was modeled successfully between two positions with an occupancy ratio of 0.75:0.25. Appropriate restraints and constraints were placed to keep the bond distances, angles, and thermal ellipsoids meaningful.

5. A solution of **5** in a mixture of dichloromethane and hexanes (1:1) was concentrated by slow evaporation. A colorless block with very well-defined faces from a representative sample of crystals of the same habit was collected and data were obtained as outlined in Table **S2**, and the structure was solved as in **1**. The X-ray radiation employed was generated from a Cu-Iμs X-ray tube (K_α = 1.5418 Å with a potential of 50 kV and a current of 1.0 mA). 45 data frames were taken at widths of 1.0°. These reflections were used to determine the unit cell. The unit cell was verified by examination of the *h k l* overlays on several frames of data. No super-cell or erroneous reflections were observed. After careful examination of the unit cell, an extended data collection procedure (28 sets) was initiated using omega and phi scans.

6. A solution of **6** in a mixture of dichloromethane and hexanes (1:1) was concentrated by slow evaporation. A colorless block with very well-defined faces from a representative sample of crystals of the same habit was collected and data were obtained as outlined in Table **S2**, and the structure was solved as in **1**. The X-ray radiation employed was generated from a Cu- X-ray sealed tube (K_α = 1.5418 Å with a potential of 50 kV and a current of 40.0 mA). 60 data frames were taken at widths of 1.0°. These reflections were used in the auto-indexing procedure to determine the unit cell. The unit cell was verified by examination of the *h k l* overlays on several frames of data. No super-cell or erroneous reflections were observed. After careful examination of the unit cell, an extended data collection procedure (3 sets) was initiated using omega scans.

Elongated ellipsoids on one *o*-Tol group (C15-C21) and the residual electron density near the group suggested disorder and was modeled successfully between two positions with an occupancy ratio of 0.94:0.06. Appropriate restraints and constraints were placed to keep the bond distances, angles, and thermal ellipsoids meaningful.

Table S1. Crystallographic data for **1**, **3**, and **4**.

	1	**3**	**4**
empirical formula	$C_{21}H_{21}OP$	$C_{27}H_{33}O_5P$	$C_{27}H_{33}O_5P$
formula weight	320.35	468.50	468.50
temperature [K]	110.0	110.0	110.0
diffractometer	Bruker Quest	Bruker Quest	Bruker APEX II
wavelength [Å]	0.71073	0.71073	0.71073
crystal system	trigonal	monoclinic	monoclinic
space group	*R*-3	$P2_1/n$	$P2_1/n$
unit cell dimensions:			
a [Å]	12.4223(6)	12.6252(4)	9.3858(15)
b [Å]	12.4223(6)	12.7293(4)	17.367(3)
c [Å]	19.7979(11)	15.4253(5)	15.469(3)
α [°]	90	90	90
β [°]	90	98.9660(10)	101.076(2)
γ [°]	120	90	90
V [Å^3]	2645.8(3)	2448.71(14)	2474.4(7)
Z	6	4	4
ρ_{calc} [Mg/m^3]	1.206	1.271	1.258
μ [mm^{-1}]	0.158	0.148	0.146
F(000)	1020	1000	1000
crystal size [mm^3]	0.459 × 0.402 × 0.259	0.527 × 0.351 × 0.327	0.403 × 0.358 × 0.341
Θ limit [°]	2.796 to 27.463	2.085 to 27.478	2.632 to 23.997
index range (*h*, *k*, *l*)	–16, 16; –16, 16; –25, 25	–16, 16; –16, 16; –20, 19	–10, 10; –19, 19; –17, 17
reflections collected	10958	54167	22281
independent reflections	1354	5595	3860
R(int)	0.0343	0.0512	0.0297
completeness to Θ	99.7 %	99.9 %	99.4 %
max. and min. transmission	0.4305 and 0.3923	0.4286 and 0.4002	0.7450 and 0.6568
data/restraints/parameters	1354 / 0 / 71	5595 / 0 / 301	3860 / 334 / 360
goodness-of-fit on F^2	1.085	1.022	1.066
R indices (final) [$I > 2\sigma(I)$]			
R_1	0.0368	0.0373	0.0460
wR_2	0.0844	0.0881	0.0979
R indices (all data)			
R_1	0.0421	0.0494	0.0521
wR_2	0.0890	0.0944	0.1010
largest diff. peak and hole [eÅ^{-3}]	0.313 and -0.381	0.343 and -0.302	0.326 and -0.338

Table S2. Crystallographic data for **5** and **6**.

	5	**6**
empirical formula	$C_{28}H_{35}O_5P$	$C_{28}H_{35}O_5P$
formula weight	482.53	482.53
temperature [K]	110.0	110.0
diffractometer	Bruker Venture	Bruker APEX II
wavelength [Å]	1.54178	0.71073
crystal system	monoclinic	monoclinic
space group	$P2_1/n$	$P2_1/n$
unit cell dimensions:		
a [Å]	12.5053(5)	10.5015(14)
b [Å]	13.0669(5)	10.0377(14)
c [Å]	15.4366(6)	24.760(3)
α [°]	90	90
β [°]	98.165(2)	98.9405(15)
γ [°]	90	90
V [Å^3]	2496.86(17)	2578.2(6)
Z	4	4
ρ_{calc} [Mg/m^3]	1.284	1.243
μ [mm^{-1}]	1.272	0.142
F(000)	1032	1032
crystal size [mm^3]	0.382 × 0.044 × 0.035	0.322 × 0.266 × 0.204
Θ limit [°]	4.265 to 70.039	2.625 to 24.996
index range (h, k, l)	–15, 15; –14, 15; –18, 18	–12, 12; –11, 11; –28, 29
reflections collected	22061	18831
independent reflections	4702	4527
R(int)	0.0313	0.0346
completeness to Θ	99.8 %	99.7 %
max. and min. transmission	0.4684 and 0.3815	0.7456 and 0.7025
data/restraints/parameters	4702 / 0 / 310	4527 / 340 / 375
goodness-of-fit on F^2	1.082	1.024
R indices (final) [$I > 2\sigma(I)$]		
R_1	0.0387	0.0347
wR_2	0.0966	0.0769
R indices (all data)		
R_1	0.0451	0.0451
wR_2	0.1041	0.0834
largest diff. peak and hole [eÅ^{-3}]	0.389 and -0.231	0.308 and -0.302

References

[S1] Bruker (2015), *APEX3*, Bruker AXS Inc., Madison, Wisconsin, USA.

[S2] Bruker (2001), *SADABS*, Bruker AXS Inc., Madison, Wisconsin, USA.

[S3] G. M. Sheldrick (2008), *XT*, *XS* Acta Cryst. A64, 112-122. G. M. Sheldrick (2015), Acta Cryst. A71, 3-8. G. M. Sheldrick (2015), Acta Cryst. C71, 3-8. BRUKER AXS Inc., 5465 East Cheryl Parkway, Madison, WI 53711-5373 USA.

[S4] The refinement was stabilized (zero shift) before the H atoms were added to the OOH groups. The latter H atoms were placed in one of the following ways: (a) If residual electron densities accounting for the corresponding H atoms were found, they were assigned as H atoms, and then were set riding on the parent O atoms. (b) If the H atoms could not be located from residual electron densities, they were placed geometrically with respect to the O atoms they were hydrogen-bonded to, and then were set riding on the parent O atoms. The last step was carried out after all remaining atoms were stabilized, and confirming there were no major shifts in those atoms after the addition of the hydrogen atoms in question.

[S5] A. L. Spek (2009), *PLATON*, Acta Cryst. D**65**, 148-155.

[S6] O. V. Dolomanov, L. J. Bourhis, R. J. Gildea, J. A. K. Howard, H. J. Puschmann (2009), *OLEX2*, Appl. Cryst., **42**, 339-341.

[S7] R. Taylor, C. F. Macrae (2001), *Mercury*, Acta Cryst., B**57**, 815-827.

Dynamic NMR Experiments

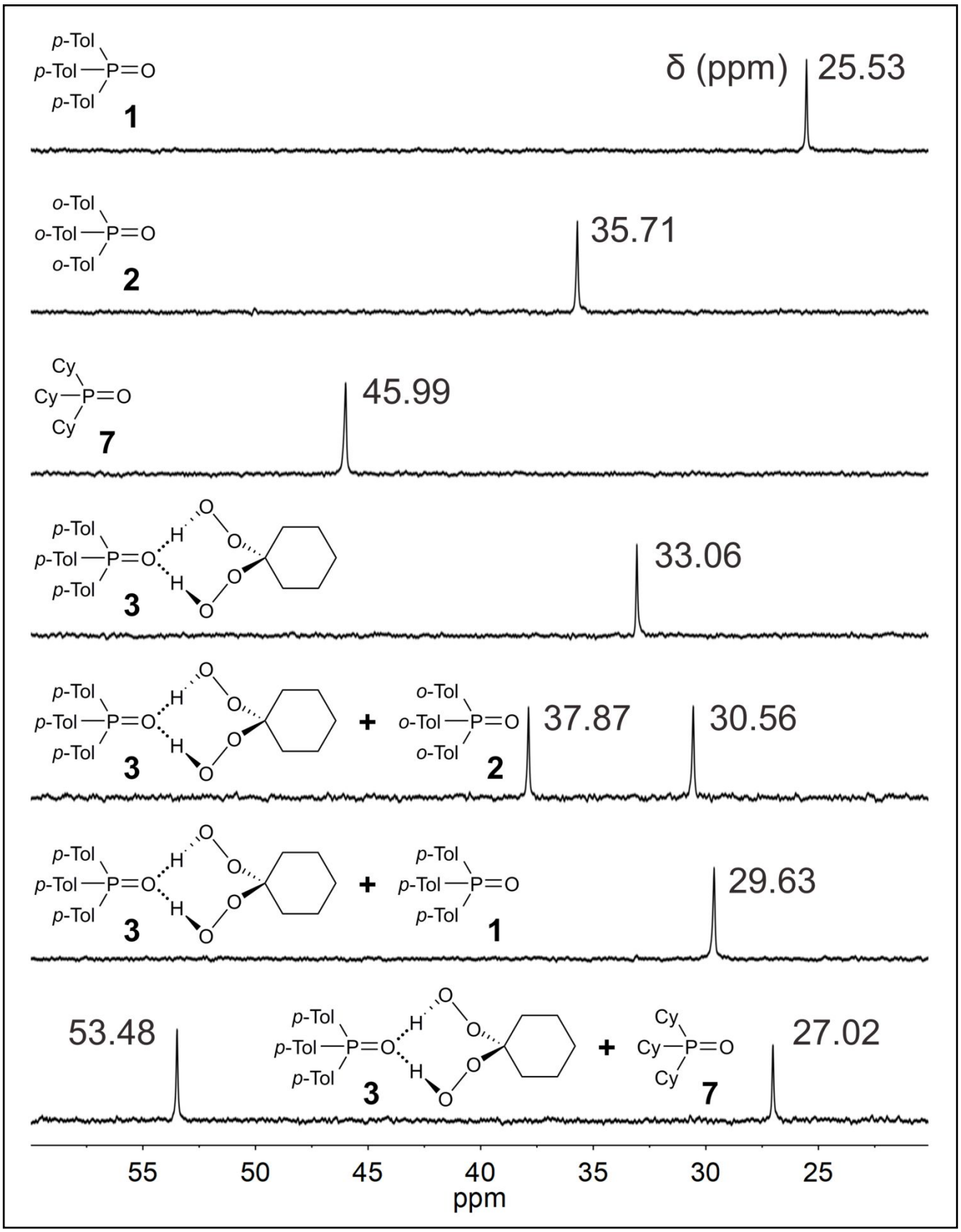

Figure S1. ^{31}P NMR competition experiments of 1 : 1 mixtures of *p*-$Tol_3PO{\cdot}(HOO)_2C(CH_2)_5$ (**3**) and phosphine oxides *p*-Tol_3PO (**1**), *o*-Tol_3PO (**2**), and Cy_3PO (**7**) in benzene.

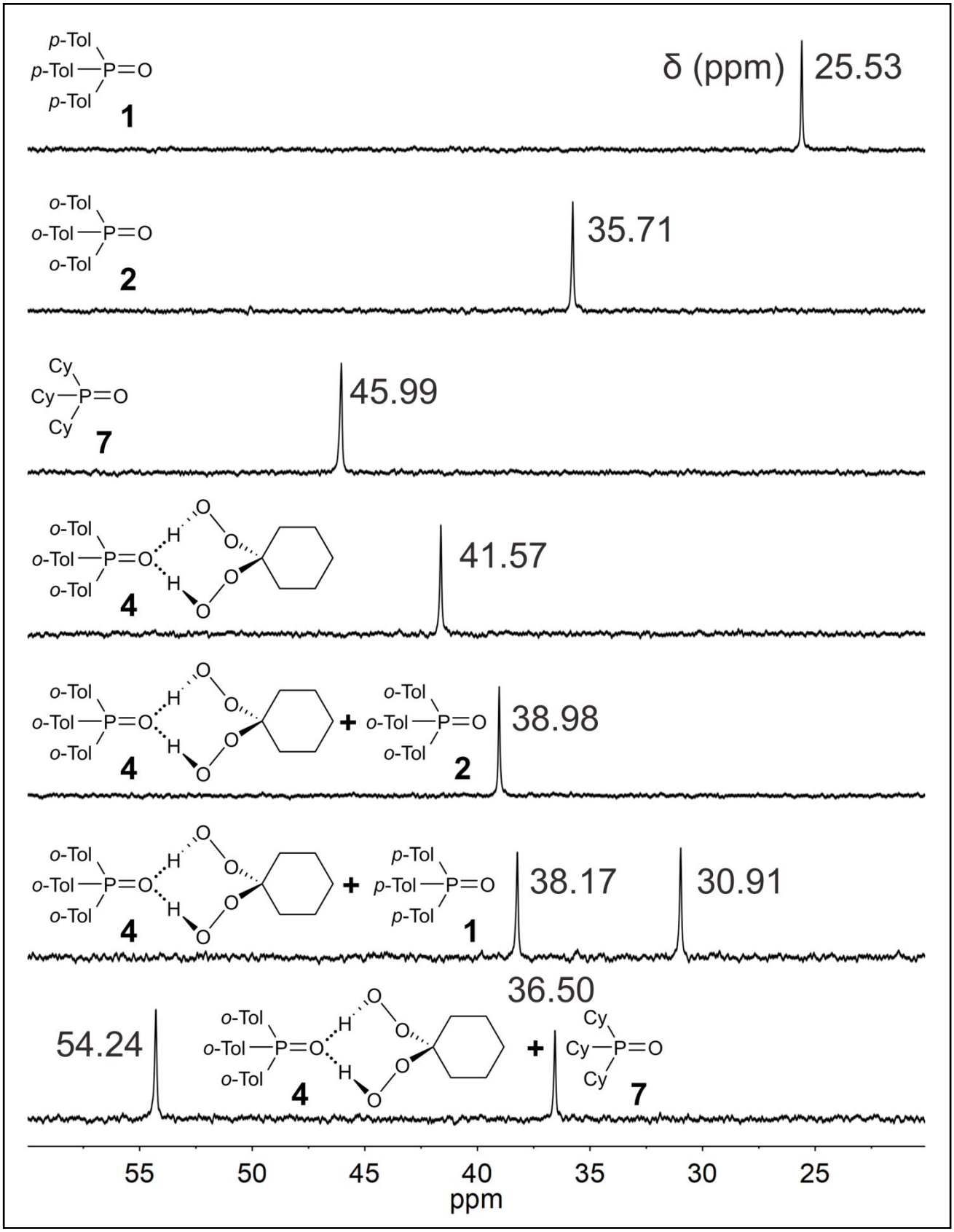

Figure S2. ^{31}P NMR competition experiments of 1 : 1 mixtures of *o*-$Tol_3PO{\cdot}(HOO)_2C(CH_2)_5$ (**4**) and phosphine oxides *p*-Tol_3PO (**1**), *o*-Tol_3PO (**2**), and Cy_3PO (**7**) in benzene.

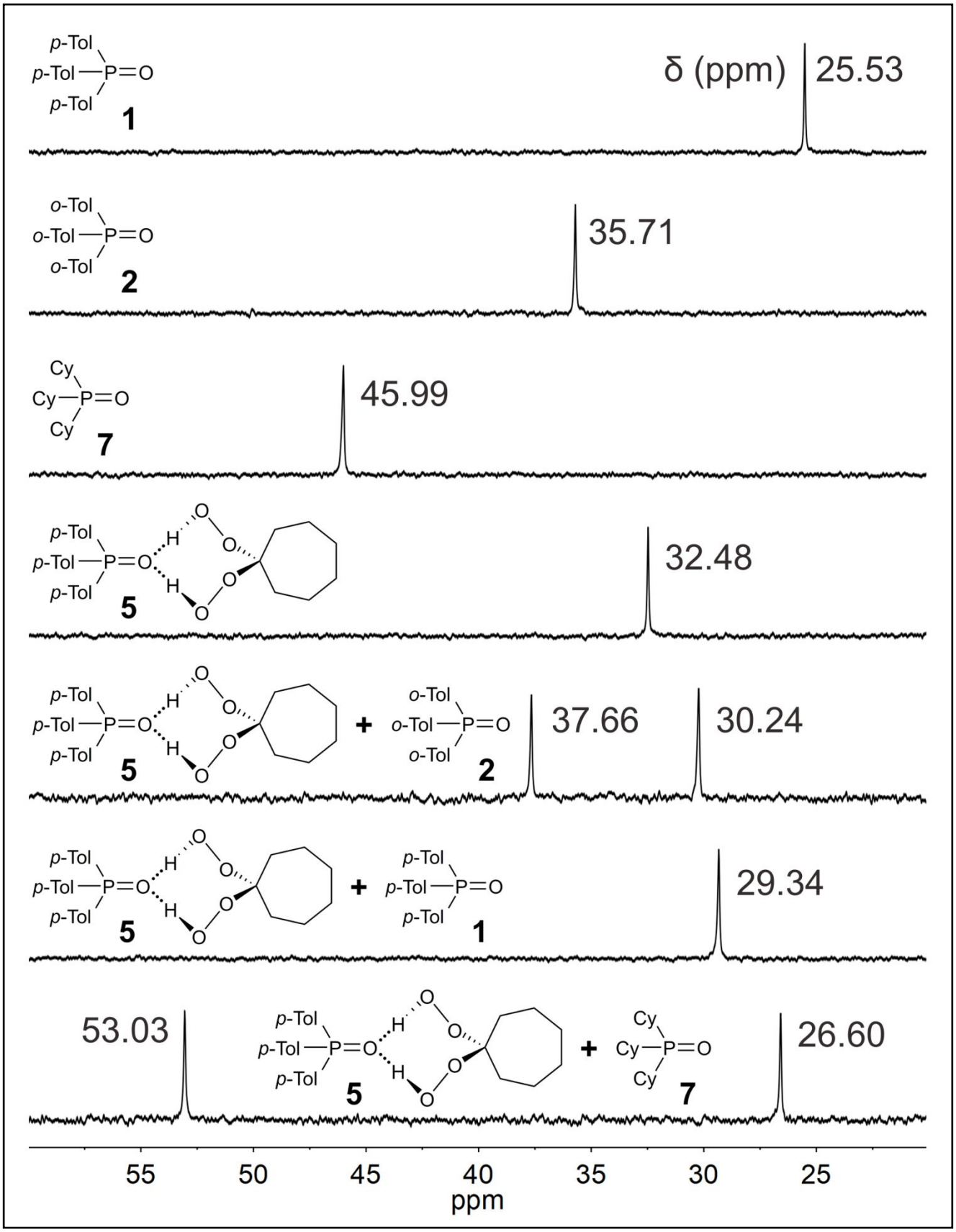

Figure S3. ^{31}P NMR competition experiments of 1 : 1 mixtures of *p*-$Tol_3PO{\cdot}(HOO)_2C(CH_2)_6$ (**5**) and phosphine oxides *p*-Tol_3PO (**1**), *o*-Tol_3PO (**2**), and Cy_3PO (**7**) in benzene.

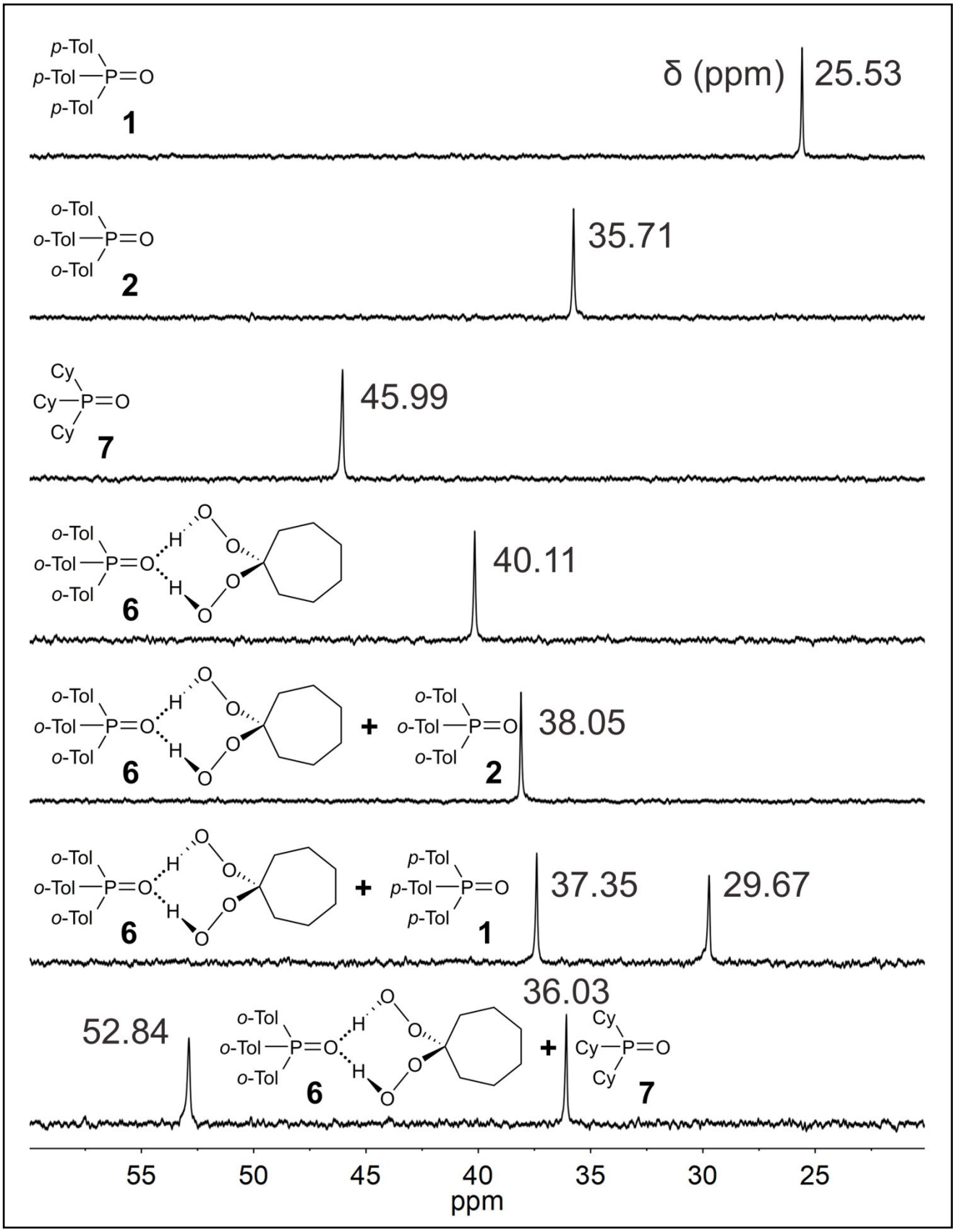

Figure S4. ^{31}P NMR competition experiments of 1 : 1 mixtures of *o*-$Tol_3PO{\cdot}(HOO)_2C(CH_2)_6$ (**6**) and phosphine oxides *p*-Tol_3PO (**1**), *o*-Tol_3PO (**2**), and Cy_3PO (**7**) in benzene.

Variable Temperature NMR experiments with a 1 : 1 ratio of adduct to phosphine oxide

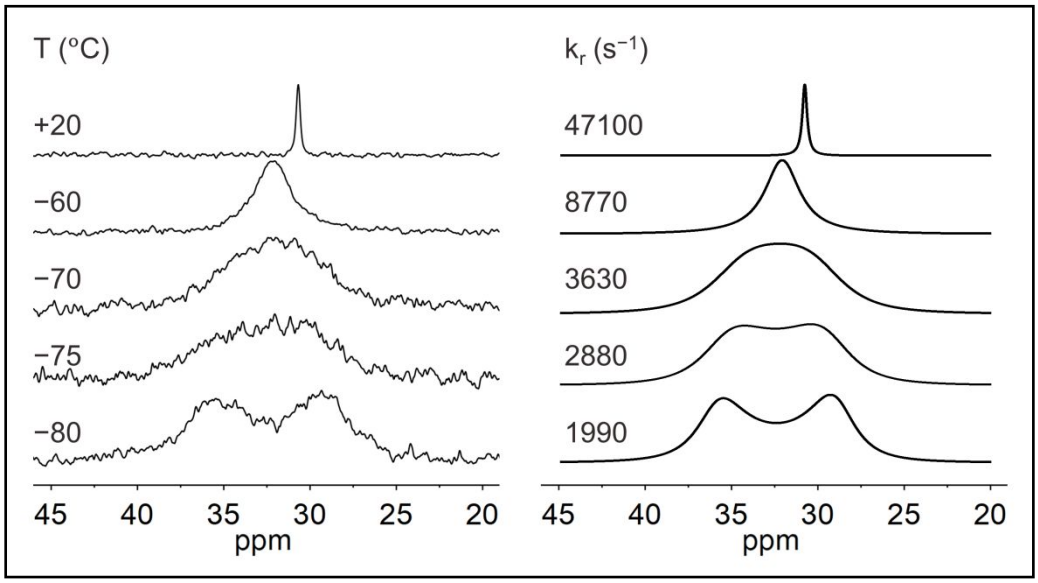

Figure S5. ^{31}P NMR spectra of a 1 : 1 mixture of *p*-Tol_3PO (**1**) and *p*-$Tol_3PO{\cdot}(HOO)_2C(CH_2)_5$ (**3**) in dichloromethane, recorded at varying temperatures (left) and the corresponding simulations (right).

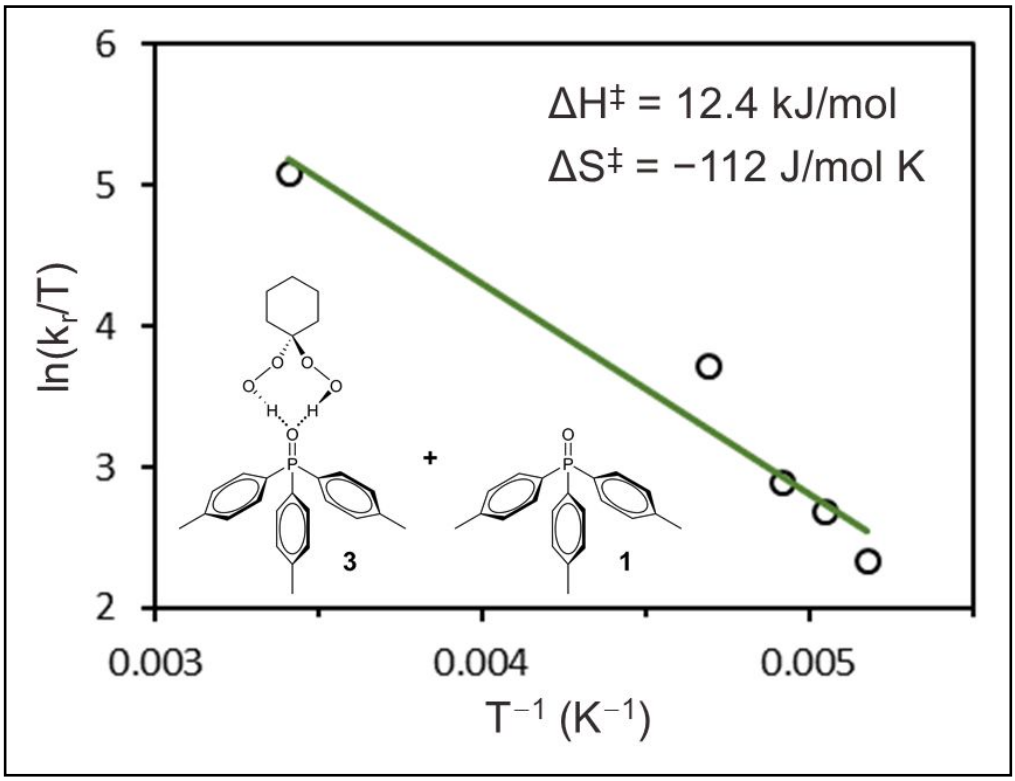

Figure S6. Temperature dependence of the exchange rate constant k_r depicted as $\ln(k_r/T)$ versus T^{-1} of a 1 : 1 mixture of *p*-Tol_3PO (**1**) and *p*-$Tol_3PO{\cdot}(HOO)_2C(CH_2)_5$ (**3**) in dichloromethane.

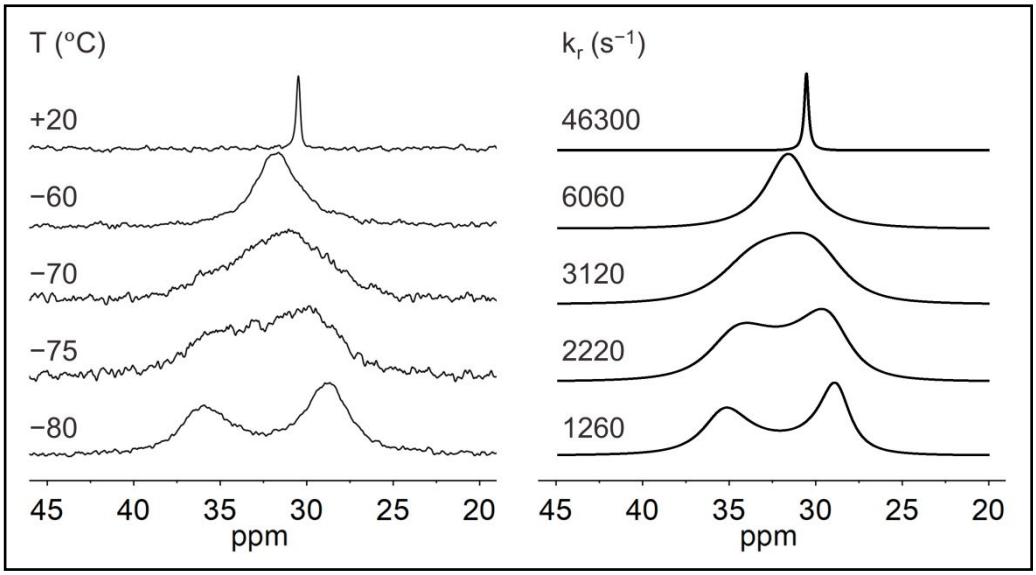

Figure S7. ^{31}P NMR spectra of a 1 : 1 mixture of *p*-Tol_3PO (**1**) and *p*-$Tol_3PO{\cdot}(HOO)_2C(CH_2)_6$ (**5**) in dichloromethane, recorded at varying temperatures (left) and the corresponding simulations (right).

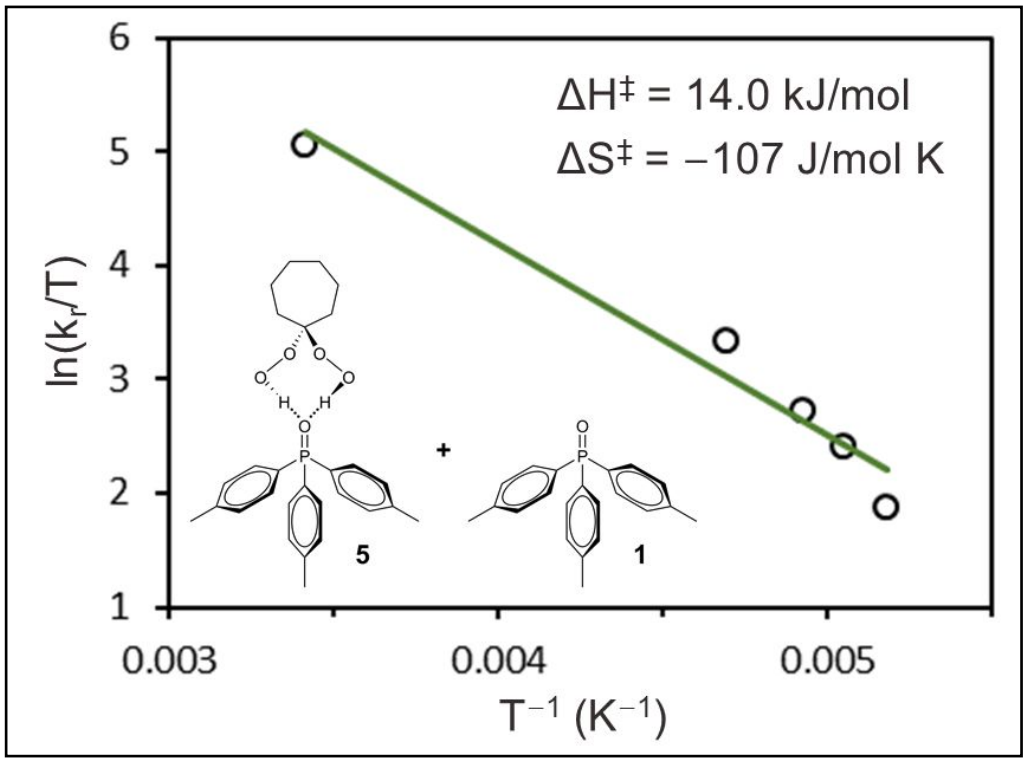

Figure S8. Temperature dependence of the exchange rate constant k_r depicted as $\ln(k_r/T)$ versus T^{-1} of a 1 : 1 mixture of *p*-Tol_3PO (**1**) and *p*-$Tol_3PO{\cdot}(HOO)_2C(CH_2)_6$ (**5**) in dichloromethane.

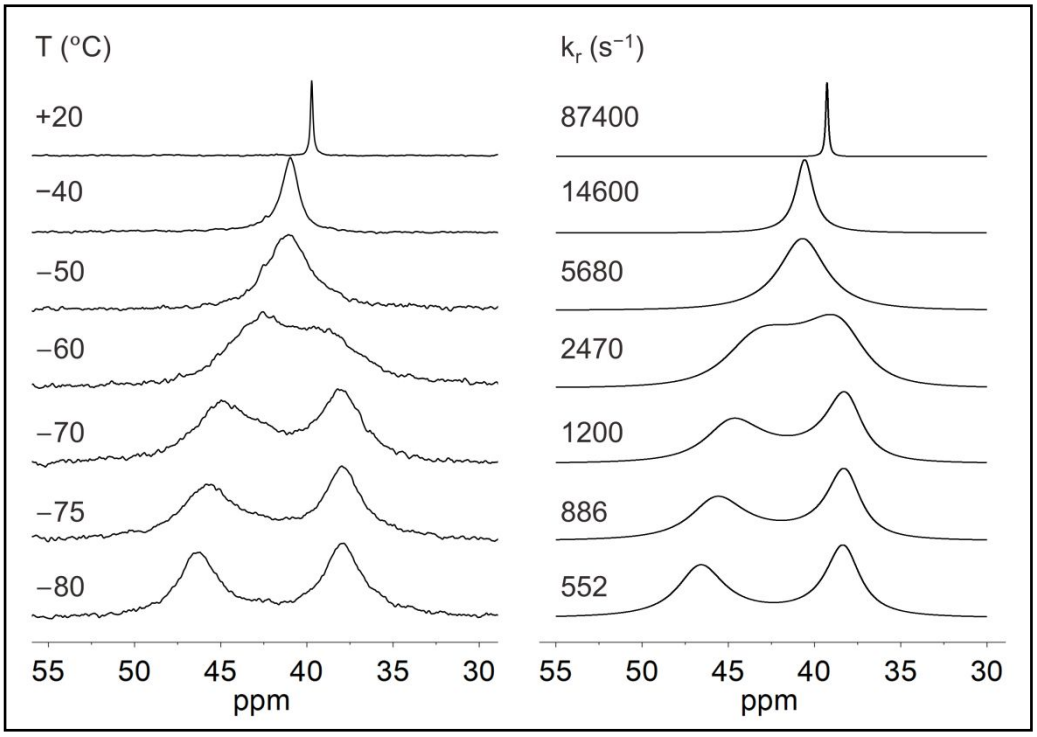

Figure S9. ^{31}P NMR spectra of a 1 : 1 mixture of *o*-Tol_3PO (**2**) and *o*-$Tol_3PO{\cdot}(HOO)_2C(CH_2)_6$ (**6**) in dichloromethane, recorded at varying temperatures (left) and the corresponding simulations (right).

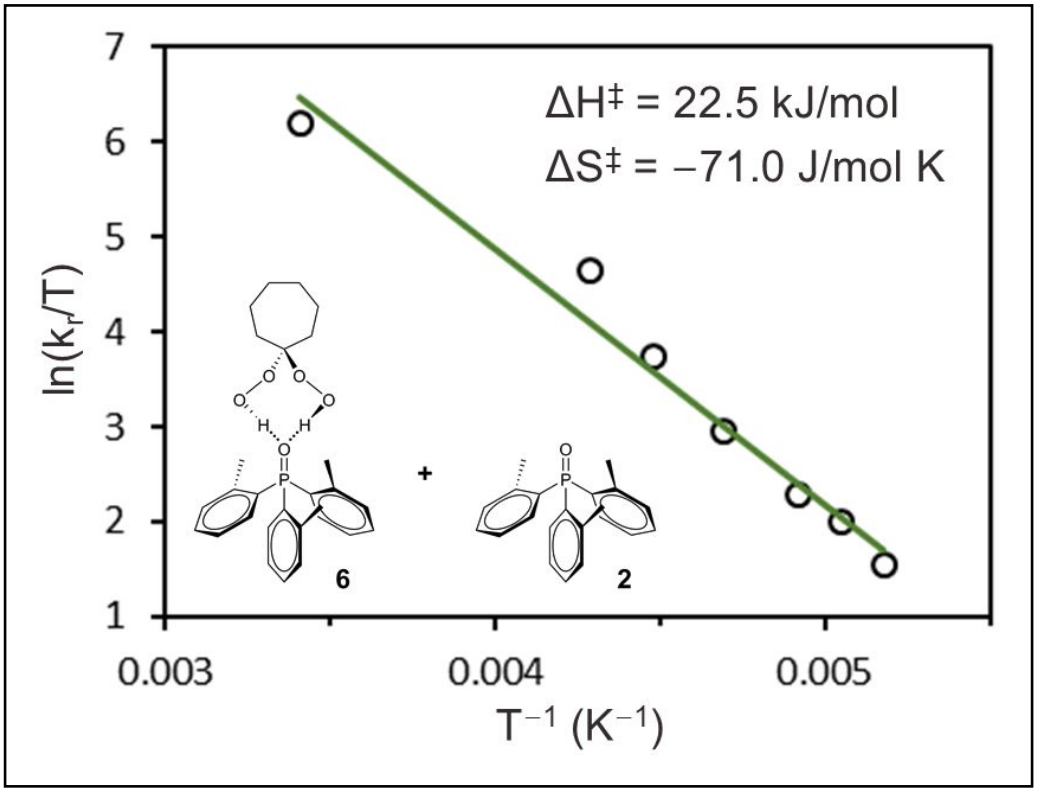

Figure S10. Temperature dependence of the exchange rate constant k_r depicted as $\ln(k_r/T)$ versus T^{-1} of a 1 : 1 mixture of *o*-Tol_3PO (**2**) and *o*-$Tol_3PO{\cdot}(HOO)_2C(CH_2)_6$ (**6**) in dichloromethane.

Table S3. ^{31}P NMR chemical shifts $\delta(^{31}P)$ (ppm) (signal halfwidths $\Delta\nu_{1/2}$ (Hz)) of the phosphine oxides **1** and **2** and adducts **3-6** in dichloromethane at the given temperatures.

T (°C)	**1**	**2**	**3**	**4**	**5**	**6**
+20	27.74 (14.4)	36.78 (21.9)	33.88 (16.3)	41.79 (17.3)	33.40 (14.8)	40.84 (17.8)
−40	28.31 (35.0)	37.31 (46.0)	−	43.81 (70.0)	−	42.43 (140.1)
−50	28.35 (28.7)	37.45 (52.3)	−	44.07 (120.3)	−	42.71 (330.8)
−60	28.40 (43.7)	37.64 (90.9)	35.85 (58.7)	44.38 (235.6)	35.02 (123.1)	*
−70	28.60 (38.6)	37.97 (140.3)	36.12 (57.0)	45.05 (431.6)	35.30 (160.8)	*
−75	28.64 (43.6)	38.14 (200.7)	36.19 (65.2)	45.84 (573.9)	35.41 (199.1)	*
−80	28.61 (42.9)	38.25 (309.7)	36.28 (75.7)	46.67 (486.11)	35.59 (254.4)	*

*Spectra were affected by exchange of **6** with a trace impurity of **2** and therefore the corresponding values of **4** were used in exchange simulations of mixture **2**/**6**.